HHS Public Access

Author manuscript

Free Radic Biol Med. Author manuscript; available in PMC 2019 August 01.

Published in final edited form as:

Free Radic Biol Med. 2018 August 01; 123: 72–84. doi:10.1016/j.freeradbiomed.2018.05.068.

Cholesterol crystals increase vascular permeability by inactivating SHP2 and disrupting adherens junctions

Arul M. Mani, **Rima Chattopadhyay**, **Nikhlesh K. Singh**, and **Gadiparthi N. Rao**

Department of Physiology, University of Tennessee Health Science Center, Memphis, TN 38163, USA

Abstract

To understand the adverse effects of cholesterol crystals on vascular homeostasis, we have studied their effects on endothelial barrier function. Cholesterol crystals increased endothelial barrier permeability in a dose and time dependent manner. In addition, cholesterol crystals induced tyrosine phosphorylation of VE-cadherin and α-catenin, disrupting endothelial AJ and its barrier function and these effects required xanthine oxidase-mediated H_2O_2 production, SHP2 inactivation and Frk activation. Similarly, feeding C57BL/6 mice with cholesterol-rich diet increased xanthine oxidase expression, H_2O_2 production, SHP2 inactivation and Frk activation leading to enhanced tyrosine phosphorylation of VE-cadherin and α-catenin, thereby disrupting endothelial AJ and increasing vascular permeability. Resolvin D1, a specialized proresolving mediator, prevented all these adverse effects of cholesterol crystals and cholesterol-rich diet in endothelial cells and mice, respectively. Based on these observations, it is likely that cholesterol crystals via disrupting AJ increase vascular permeability, a critical event of endothelial dysfunction and specialized proresolving mediators such as Resolvin D1 exert protection against these effects.

INTRODUCTION

Endothelial cells are involved in the maintenance of vessel integrity, vascular tone and vascular permeability as well as prevention of vascular inflammation and thrombosis [1–3]. Intercellular junctions between endothelial cells maintain vascular integrity and its barrier function [4–7]. Under physiological conditions, the endothelial barrier function is tightly regulated and vascular permeability is limited [5, 6]. On the other hand, vascular pathologies such as atherosclerosis are associated with disruption of endothelial barrier function [8, 9]. Adherens junctions (AJ) and tight junctions (TJ) are the two major types of intercellular junctions that maintain endothelial barrier function [4, 5]. The steady state levels and

Address correspondence to: Gadiparthi N. Rao, Ph. D., Department of Physiology, University of Tennessee HSC, 71 S. Manassas Street, Memphis, TN 38163, USA, Phone: 901-448-7321, Fax: 901-448-7126, rgadipar@uthsc.edu.

AUTHORS CONTRIBUTIONS

AMM, performed flux assay, TER, Western blotting, coimmunoprecipitation, H_2O_2 release, SHP2 activity and fed mice with CRD in combination with and without RvD1; RC, performed flux assay, TER, Western blotting, and immunofluorescence staining; NKS, performed Miles assay and immunofluorescence staining; GNR conceived the overall goal of the project, designed the experiments, interpreted the data and wrote the manuscript.

CONFLICT OF INTEREST

None

posttranslational modifications such as phosphorylation of AJ and TJ proteins determine their stability and are involved in the regulation of vascular permeability [10–16]. AJ are composed of a transmembrane protein namely, vascular endothelial (VE)-cadherin and its binding partners α-, β-, γ-, and p120-catenins [4–6]. Besides its association with catenins, VE-cadherin interacts with actin-binding proteins via α-catenin and thus plays a crucial role in the maintenance of cell-to-cell junction and cytoskeleton stability [4, 5, 7, 17]. In recent years, various laboratories have reported the presence of cholesterol crystals in human atherosclerotic plaques [18–20]. It was also reported that cholesterol crystals promote plaque vulnerability and rupture [20, 21]. In addition, it was shown that cholesterol crystals induce NLRP3 inflammasome formation [22]. Furthermore, inhibition of NLRP3 inflammasome formation attenuated atherosclerosis [23]. Besides, studies from our laboratory showed that cholesterol crystals induce foam cell formation [24]. Although the presence of cholesterol crystals in various stages of atherogenesis and their capacity in stimulating NLRP3 inflammasome formation and foam cell formation have been reported [18–22, 24], the adverse effects of these crystals on vascular function at large are less clear. Since endothelial dysfunction is an early event in the development of atherosclerosis [25, 26], we asked the question whether cholesterol crystals affect endothelial function. To address this assumption, in the present study we have tested the effects of cholesterol crystals on endothelial AJ integrity and its barrier function. Our findings reveal that cholesterol crystals trigger XO-mediated H_2O_2 production, SHP2 cysteine oxidation and its inactivation, Frk activation and VE-cadherin and α-catenin tyrosine phosphorylation and their dissociation from each other leading to AJ disruption and increased endothelial barrier permeability. In addition, we found that RvD1, a specialized proresolving mediator, protects endothelial AJ and its barrier function from cholesterol crystals-induced disruption. Furthermore, feeding mice with cholesterol-rich diet (CRD) also induced xanthine oxidase expression, H_2O_2 production, SHP2 cysteine oxidation and its inactivation, Frk activation, VE-cadherin and α-catenin tyrosine phosphorylation affecting AJ integrity and vascular permeability and RvD1 attenuated all these adverse effects of CRD feeding substantially.

MATERIALS AND METHODS

Reagents:

Anti-VE-cadherin (SC-9989), anti-α-catenin (SC-9988), anti-β-catenin (SC-7199), anti-p120 catenin (SC-23872), anti-Frk (SC-166478) and anti-α-tubulin (SC-23948) antibodies were purchased from Santa Cruz Biotechnology Inc., (Santa Cruz, CA). Resolvin D1 (10012554) was obtained from Cayman Chemical Company (Ann Arbor, MI). Fluorescein isothiocyanate-dextran (FD70S) and PHPS1 (P0039) were bought from Sigma Aldrich Company (St. Louis, MO). Anti-PY20 (05–777) antibodies and PTP assay kit (17–125) were obtained from Millipore (Temecula, CA). Anti-SHP2 (610622) antibodies were purchased from BD Biosciences (San Jose, CA). Anti-cysteine sulfonate antibody (ADI-OSA-820-F) was bought from Enzo Life Sciences (Farmingdale, NY). HRP-conjugated goat anti-rabbit (31460) and goat anti-mouse (31437) secondary antibodies, anti-VE-cadherin (MA1–198), Hoechst 33342 (10 mg/ml) solution (H3570), Alexa Fluor 568 goat anti-mouse (A11004), Alexa Fluor 488 goat anti-mouse (A11001), fluorochrome secondary antibodies, ProLong Gold antifade reagent (P36930), Medium 200 (M200500), low serum growth supplements

(S003K), Lipofectamine 3000 (L3000015), non-targeting siRNA (D-001810–10), Frk siRNA (S5363), and gentamycin/amphotericin solution (R01510) were bought from ThermoFisher Scientific (Carlsbad, CA). The enhanced chemiluminescence (ECL) Western blotting detection reagents (RPN2106) was obtained from GE Healthcare Life Sciences (Pittsburg, PA).

Cell culture:

Human aortic endothelial cells (HAECs) (Cat. No. H6052) were purchased from Cell Biologics (Chicago, IL) and cultured in Medium 200 containing low serum growth supplements (LSGS), 10 μg/ml gentamycin and 0.25 μg/ml amphotericin B. Cultures were maintained at 37°C in a humidified 95% air and 5% CO_2 atmosphere. HAECs between 6–10 passages were growth-arrested by incubating in Medium 200 without LSGS for 6 hrs and used to perform the experiments unless otherwise indicated.

Animals:

C57BL/6 mice were purchased from Charles River Laboratories (Wilmington, MA). Mice were maintained at UTHSC vivarium according to the Institutional Animal Care and Use Committee's guidelines. The experiments involving animals were approved by the Animal Care and Use Committee of the University of Tennessee Health Science Center, Memphis, TN. To study the effect of RvD1 on the protection of endothelial barrier function, mice were fed with chow diet (CD) or cholesterol-rich diet (CRD) for 12 weeks and the group of mice that were on CRD were given intraperitoneal injection of vehicle or RvD1 at a dose of 10 mg/kg body weight every third day for the entire period of the regimen. At the end of the experimental period, mice were used either to measure vascular permeability or sacrificed and aortas were isolated for further analysis as required.

Cholesterol crystal preparation:

Cholesterol crystals were prepared as described previously [24]. Briefly, twenty-five grams of anhydrous cholesterol was dissolved in 2L of prewarmed (60°C) 95% ethanol. While warm, the mixture was filtered through Whatmann-1 filter paper to remove the unwanted debris. The mixture was left overnight at room temperature and the sedimented cholesterol crystals were filtered through Whatmann-1 filter paper and dried at room temperature. The same procedure was repeated twice in order to obtain pure monohydrated cholesterol crystals. The crystals were grounded using mortar and pestle and stored in amber colored bottle at −20°C. The cholesterol crystals were used as needed.

Flux assay:

HAECs were grown to a confluent monolayer on the apical side of a 12-well Transwell (polycarbonate membrane with 0.4 mm pore size). The cells were growth-arrested for 6 hrs in serum-free Medium 200. The monolayer was treated with and without cholesterol crystals (200 mg/ml) for the indicated time periods. Wherever siRNAs were used, cells were transfected with the indicated siRNA and 36 hrs later, these cells were seeded onto the transwell. In the case of pharmacological inhibitors or RvD1, they were added 30 min prior to the addition of cholesterol crystals. Fluorescein isothiocyanate-conjugated dextran (MW

~70 kDa) was added to the top chamber (apical surface) at 100 mg/ml concentration and incubated at 37°C for 2 hrs. The fluorescence intensity of the medium from each chamber (both apical and basal) was measured using SpectraMax Gemini XPS Spectrofluorometer (Molecular Devices). Permeability coefficient of dextran flux was calculated by using the following equation: Po = (F1/ΔT) VA/FA × A, where F1 is basal fluorescence; FA is apical fluorescence; ΔT is change in time (min); A is surface area; VA is volume of basal chamber. The flux was expressed as % dextran diffused/min/cm^2.

Transendothelial electrical resistance (TER):

HAECs were seeded onto apical chamber of a 12-well Transwell (polycarbonate membrane with 0.4 mm pore size) at a density of 10^5 cells/cm^2. The cells were allowed to grow to reach a complete monolayer and then growth-arrested for 6 hrs in serum-free Medium 200. The cells were treated with and without cholesterol crystals (200 μg/ml) in the presence and absence of RvD1 (200 ng/ml) or the indicated pharmacological inhibitors for the indicated time periods. Wherever siRNAs were used, cells were transfected with the indicated siRNA and 36 hrs later, these cells were seeded onto a transwell. Resistance, as an index of barrier function, to current flow between cells and beneath the cell layer, created by cell-cell and cell-matrix components, was measured at various time periods using a Millicell ERS-2VOhm Meter (MERS00002, EMD Millipore). Transendothelial resistance was calculated using the following equation: TER= (TER at a particular time period – basal TER)/surface area of the transwell. Surface area of 12-mm inserts, which were used in this study, is approximately 1.33 cm^2. Resistance was expressed as Ω.cm^2.

H_2O_2 production assay:

HAECs with and without the indicated treatments were collected by scraping and 500 μl of the cell suspension was incubated with 50 μl of 100 μM Amplex Red along with 0.2 U/ml of HRP for 30 min at 37°C in the dark. Following the incubation, the fluorescence intensities were measured in SpectraMax Gemini XPS Spectrofluorometer (Molecular Devices) with excitation at 530 nm and emission at 590 nm. The H_2O_2 production was expressed as RFU.

Transfections:

HAECs were transfected with the indicated siRNA at a final concentration of 100 nM using Lipofactamine 3000 transfection reagent according to the manufacturer's instructions. After transfections, cells were quiesced in Medium 200 without LSGS for 6 hrs and used as required.

Immunoprecipitation:

Immunoprecipitation was performed as described by us previously [16]. Cell or tissue extracts containing equal amounts of protein from control and the indicated treatments was incubated with the indicated primary antibody at 1:100 dilution overnight at 4°C. Protein A/G-conjugated Sepharose CL-4B beads were added and incubation continued for an additional 1 hr at room temperature and the beads were collected by centrifugation at 1000 rpm for 1 min at 4°C. The beads were washed three times with lysis buffer and once with PBS, boiled in SDS sample buffer and analyzed by immunoblotting.

Western blot analysis:

Cell or tissue extracts containing equal amounts of protein from control and the indicated treatments were resolved by SDS-PAGE. The proteins were transferred electrophoretically to a nitrocellulose membrane. After blocking in either 5% (W/V) nonfat dry milk or 5% (W/V) BSA, the membrane was probed with appropriate primary antibodies followed by incubation with horseradish peroxidase-conjugated secondary antibodies. The antigen-antibody complexes were detected using enhanced chemiluminescence detection reagents.

Immunofluorescence:

HAECs were grown to a confluent monolayer on cell culture grade glass cover slips, quiesced and treated with and without cholesterol crystals (200 mg/ml) in the presence and absence of RvD1 (200 ng/ml) alone or in combination with the indicated inhibitors for the indicated time periods. After the treatments, cells were washed with cold PBS, fixed with 95% ethanol for 30 min at 4°C, permeabilized in TBS (10 mM Tris-HCl, pH 8.0, 150 mM NaCl) containing 0.1% Triton X-100 for 10 min at room temperature and blocked with 2% BSA in TBS containing 10 mM $CaCl_2$, 5 mM $MgCl_2$ and 0.1 % saponin overnight at 4°C. After incubation with appropriate primary antibodies (1:200 dilution), Alexa Flour-conjugated secondary antibodies were added (1:500 dilution) and incubation continued for 1 hr at room temperature, counter stained with Hoechst 33342 (1:3000 dilution in PBS) for 2 min at room temperature and mounted onto glass slides with Prolong Gold antifade mounting medium. In the case of aortas, after dissection they were cleaned from fat tissue, opened longitudinally, fixed with 2% paraformaldehyde for 1 hr, permeabilized with 0.2 % Triton-X-100 in PBS for 20 min and blocked in PBS containing 0.1 % Triton-X-100 and 5% FBS for 1 hr at room temperature before being incubated with primary and secondary antibodies. Fluorescence images of the cells and aortas were captured using an inverted Zeiss fluorescence microscope (AxioObserver Z1) via a 40X (NA 0.6) objective and AxioCam MRm camera without any enhancements using the microscope operating and image analysis software AxioVision Version 4.7.2 (Carl Zeiss Imaging Solutions GmbH).

SHP2 assay:

Cell or tissue extracts containing equal amounts of protein from control and the indicated treatments were immunoprecipitated with anti-SHP2 antibodies at 1:100 dilution overnight at 4°C. Protein A/G-conjugated Sepharose CL-4B beads were added (50 μl of 50% slurry) and incubation continued for an additional 3 hrs at 4°C. The beads were washed three times with 10 mM Tris-HCl, pH 7.4 containing 100 μM dithiothreitol. The washed beads were resuspended in 25 μl of 10 mM Tris-HCl, pH 7.4 and incubated with 100 μM phosphopeptide (RRLIEDAEpYAARG) substrate at room temperature for 30 min. The samples were centrifuged and the supernatants were collected. Twentyfive microliters of the supernatants were incubated with 100 ml of malachite green solution in a microwell plate for 15 min and the inorganic phosphate release was measured in Spectramax 190 spectrophotometer (Molecular Devices) at 650 nm and calculated using a free phosphate standard curve. The SHP2 activity was presented as picomoles of pi released.

Miles assay:

Vascular permeability was determined by quantitative measurement of the Evans Blue dye diffusion into the aorta as described previously using Miles assay [16]. Briefly, WT mice that were fed with CRD in combination with and without RvD1 (10 μg/kg body weight) for 12 weeks were anesthetized, and 0.1 ml of 1% Evans Blue dye was injected into the inferior vena cava. After 30 min, blood vessels were perfused with PBS through the left ventriculum and aortas were isolated and pictures were taken using Nikon SLR camera (Model D7100). Then, Evans Blue dye was extracted from the arteries by incubating in formaldehyde at 55°C for 24 hrs, cleared by centrifugation and the optical density was measured at 610 nm. Vascular permeability was expressed as the amount of Evans Blue extravasated per mg artery.

Statistics:

All the experimental data was presented as Mean ± SD. The treatment effects were evaluated by one way analysis of variance (ANOVA) followed by Bonferroni's multiple comparison tests. A value of $p < 0.05$ was considered to be statistically significant.

RESULTS

Cholesterol crystals induce HAEC barrier dysfunction

Many studies have demonstrated the presence of cholesterol crystals in atherosclerotic plaques and their capacity to trigger inflammasome formation [9, 18–22]. A few studies have also shown that formation of cholesterol fatty streaks as one of the major factors in the development of atherosclerosis [9, 27]. But the underlying mechanisms of inflammation and atherosclerotic lesion progression by cholesterol crystals are just begun to be unfolded [22–24]. As endothelial dysfunction [25, 26] and inflammation [28] are linked to the development of atherosclerosis and to understand the potential mechanisms by which cholesterol crystals may influence these events, we tested the effect of cholesterol crystals on endothelial barrier function. Cholesterol crystals increased dextran flux in a dose and time dependent manner compared to vehicle control (Figure 1A & B). Consistent with these observations, cholesterol crystals decreased transendothelial resistance (TER) (Figure 1C). These results indicate that cholesterol crystals disrupt endothelial barrier function. Since AJ play an important role in the maintenance of endothelial barrier function and to understand the mechanisms by which cholesterol crystals disrupt endothelial barrier function, we first tested the effect of cholesterol crystals on the steady state levels of AJ proteins, namely VE-cadherin, α-catenin, β-catenin and p120-catenin. Cholesterol crystals had no effect on the steady state levels of VE-cadherin, α-catenin, β-catenin and p120-catenin over a period of 4 hrs (Figure 1D). As cholesterol crystals disrupted the endothelial barrier function without altering the steady state levels of AJ proteins, we reasoned that cholesterol crystals might be disrupting AJ by posttranslational modifications of these proteins. It was reported that phosphorylation of AJ proteins regulates AJ integrity and endothelial barrier function [11, 12]. Therefore, we examined the effects of cholesterol crystals on AJ protein tyrosine phosphorylation. Cholesterol crystals while having a modest effect on p120-catenin tyrosine phosphorylation, robustly increased the tyrosine phosphorylation of VE-cadherin, α-catenin and β-catenin (Figure 1E). To understand the significance of increased tyrosine

phosphorylation of AJ proteins by cholesterol crystals, we next examined their interactions. First, α-catenin, β-catenin and p120-catenin existed in complex with VE-cadherin in quiescent cells (Figure 1F). Second, in response to cholesterol crystals, α-catenin but not β-catenin or p120-catenin dissociated from VE-cadherin (Figure 1F). Accordingly, both VE-cadherin and α-catenin were found colocalized on the cell surface of quiescent HAEC and in response to cholesterol crystals their colocalization was disintegrated as seen by double immunofluorescence staining (Figure 1G).

Frk mediates cholesterol crystals-induced HAEC barrier dysfunction

We have previously reported that Frk, a member of the Src family of protein tyrosine kinases [29], plays a role in LPS-induced AJ protein tyrosine phosphorylation leading to AJ disruption [30]. Based on these observations, we asked whether Frk is involved in the tyrosine phosphorylation of VE-cadherin and α-catenin in the disruption of AJ in response to cholesterol crystals. Cholesterol crystals induced tyrosine phosphorylation of Frk in a time dependent manner (Figure 2A). This result infers that cholesterol crystals activate Frk in HAEC. Next, we tested the role of Frk in cholesterol crystals-induced VE-cadherin and α-catenin tyrosine phosphorylation and AJ disruption. Depletion of Frk levels by its siRNA inhibited cholesterol crystals-induced VE-cadherin and α-catenin tyrosine phosphorylation and their dissociation from each other as compared to siControl (Figure 2B). Double immunofluorescence staining for VE-cadherin and α-catenin showed reappearance of their colocation on the cell surface of Frk-depleted cells as compared to siControl cells (Figure 2C). In line with these observations, depletion of Frk levels prevented cholesterol crystals-induced increases in HAEC barrier permeability and thereby restored their TER (Figure 2D & E).

Xanthine oxidase-dependent H_2O_2 production mediates cholesterol crystals-induced HAEC barrier dysfunction

Earlier studies from others as well as our laboratory have shown that ROS production is an underlying factor in endothelial cell dysfunction [30–33]. Based on these findings, we tested whether cholesterol crystals induce ROS production in the disruption of endothelial barrier function. As shown in Figure 3A, cholesterol crystals induced H_2O_2 production in a time dependent manner with maximum effect at 10 min. To identify the source of H_2O_2 production, we tested the role of xanthine oxidase. Inhibition of xanthine oxidase by Allopurinol [34] substantially blocked cholesterol crystals-induced H_2O_2 production (Figure 3B). In addition, preincubation with PEG-catalase abolished H_2O_2 production by cholesterol crystals (Figure 3B). These observations reveal that cholesterol crystals triggers H_2O_2 production via xanthine oxidase activation in HAEC. To explore the role of H_2O_2 in cholesterol crystals-induced AJ protein tyrosine phosphorylation and AJ disruption, we studied the effect of Allopurinol. Allopurinol inhibited cholesterol crystals-induced Frk, VE-cadherin and α-catenin tyrosine phosphorylation, VE-cadherin and α-catenin dissociation from each other and their disintegration from the cell surface of HAEC (Figure 3C–E). Consistent with these observations, Allopurinol also prevented cholesterol crystals-induced increases in HAEC barrier permeability and restored their TER (Figure 3F & G).

Resolvin D1 protects endothelial barrier function from cholesterol crystals-induced disruption

Resolvins, a group of specialized proresolving mediators produced by metabolic conversion of omega 3 polyunsaturated fatty acids, particularly docosahexaenoic acid and eicosapentaenoic acid have been shown to possess anti-inflammatory functions [35–37]. Since cholesterol crystals induced endothelial barrier permeability, which is implicated in the propagation of inflammation [2], we asked the question whether Resolvin D1 has any antagonistic effects to cholesterol crystals. RvD1 blocked cholesterol crystals-induced H_2O_2 production, Frk activation, VE-cadherin and α-catenin tyrosine phosphorylation and their dissociation from each other and their disintegration from the cell surface of HAEC (Figure 4A–F). In addition, RvD1 inhibited cholesterol crystals-induced increase in endothelial barrier permeability and restored their TER (Figure 4 G & H).

Role of SHP2 inactivation in cholesterol crystals-induced endothelial barrier disruption

Many studies have shown that ROS via oxidation of the catalytic cysteine residues of protein tyrosine phosphatases leads to their inactivation and thereby influences protein tyrosine kinase activation [38, 39]. Previously, we have reported that ROS mediates SHP2 cysteine oxidation and its inactivation in the modulation of LPS-induced Frk activation and AJ protein tyrosine phosphorylation leading to AJ disruption and endothelial barrier dysfunction [30]. In view of these observations, we tested the role of SHP2 in cholesterol crystals-induced Frk activation and AJ protein tyrosine phosphorylation. Cholesterol crystals induced SHP2 cysteine oxidation (Figure 5A). In addition, Allopurinol and PEG-catalase inhibited cholesterol crystals-induced SHP2 cysteine oxidation and its inactivation (Figure 5B). Similarly, RvD1 also inhibited SHP2 cysteine oxidation and its inactivation (Figure 5C). To find whether SHP2 inactivation is involved in cholesterol crystals-induced endothelial barrier dysfunction, we examined the effects of its pharmacological inhibition on the protective effects of RvD1. In the presence of SHP2 inhibitor, PHPS1 [40], RvD1 was not able to suppress cholesterol crystals-induced Frk activation, VE-cadherin and α-catenin tyrosine phosphorylation and their dissociation from each other and AJ disruption (Figure 6A & B). Similarly, in the presence of SHP2 inhibitor, RvD1 was not able to prevent cholesterol crystals-induced increases in endothelial barrier permeability and therefore failed to restore its TER (Figure 6C & D). These results infer that SHP2 mediates cholesterol crystals-induced Frk activation, VE-cadherin and α-catenin tyrosine phosphorylation and their dissociation and AJ disruption and that RvD1 exerts its protective effects on endothelial barrier function via blockade of H_2O_2 production and SHP2 oxidation and its inactivation.

CRD disrupts endothelial barrier function via oxidative inactivation of SHP2, Frk activation, AJ protein tyrosine phosphorylation and AJ disruption and RvD1 alienates these effects

To validate the in vitro observations in vivo, WT mice were fed with CRD in the presence and absence of RvD1 (10 mg/kg body weight by IP every 3rd day) or left on CD for 12 weeks and tested for XO expression, ROS production, SHP2 inactivation, Frk activation and AJ protein tyrosine phosphorylation and AJ disruption. Feeding mice with CRD for 12 weeks led to increased XO expression and H_2O_2 production (Figure 7A), SHP2 cysteine oxidation and its inactivation (Figure 7B), Frk activation (Figure 7C) and AJ protein tyrosine

phosphorylation and their dissociation (Figure 7C). According to these observations, CRD feeding also led to AJ disruption and increased vascular permeability (Figure 7D & E). Interestingly, RvD1 inhibited all these adverse effects of CRD feeding on XO expression and H_2O_2 production, SHP2 cysteine oxidation and its inactivation, Frk activation, AJ protein tyrosine phosphorylation and their dissociation, AJ disruption and vascular permeability (Figure 7A–E).

DISCUSSION

High blood cholesterol levels are considered as a major risk factor for cardiovascular diseases including plaque formation in the arteries leading to the development of atherosclerosis [27]. In addition, many studies have shown the presence of cholesterol crystals in the atherosclerotic plaques [18–21]. Interestingly, feeding mice with high fat diet led to generation and appearance of cholesterol crystals in the sinus [9]. Cholesterol crystals have also been reported to trigger inflammasome formation, which is involved in the production of proinflammatory cytokines [22]. Since inflammation plays an essential role in the development of atherosclerosis [28], the presence of cholesterol crystals in the plaques and its capacity to stimulate inflammasome formation can be indeed viewed cholesterol crystals as a causative factor in the development of atherosclerosis. Although there is mounting evidence for the involvement of cholesterol crystals in atherosclerosis (9, 18–21, 27], the underlying mechanisms by which cholesterol crystals influence the pathogenesis of atherosclerosis are just beginning to be unfolded [22]. Towards this end, previously we have reported that cholesterol crystals induce foam cell formation [24], whose build up in the artery leads to lesion progression [41]. Since endothelial dysfunction is an early event in atherosclerosis [25, 26], we asked the question whether cholesterol crystals affect endothelial function. In the present study, we show that cholesterol crystals increase vascular permeability. Endothelial cell-to-cell junctions, namely AJ and TJ, play a crucial role in the modulation of vascular permeability [4, 5]. Disruption of these cell-to-cell contacts increases vascular permeability and affects endothelial function [8, 9]. VE-cadherin is a transmembrane protein of AJ and exists in complex with a large number of intracellular molecules including α-catenin, β-catenin, α-catenin and p120 catenin [4, 5]. It also interacts with actin-binding proteins such as vinculin [42]. Its interaction with actin-binding proteins is critical for its role in the maintenance of the cytoskeleton and cell-to-cell junction stability [17]. More interestingly, VE-cadherin interacts with actin-binding proteins via α-catenin [17]. In addition, many signaling molecules such as protein tyrosine kinases and protein tyrosine phosphatases have been found to be associated with VE-cadherin [43–45]. Based on its interactions with various proteins, it could be speculated that VE-cadherin could be a target of intense regulation by various cues in the modulation of vascular permeability. Therefore, changes in its steady state levels or function could affect the overall stability of the endothelial cell-to-cell junctions and cytoskeleton. In fact, previous studies from other laboratories have demonstrated that phosphorylation-dependent VE-cadherin internalization and degradation leads to AJ disruption and increased endothelial barrier permeability [46]. Along with these observations, in the present study we show that cholesterol crystals increase tyrosine phosphorylation of VE-cadherin and α-catenin leading to their dissociation from each other, thereby affecting endothelial AJ integrity and barrier function. Previously,

we have reported that LPS stimulates Frk activation in the phosphorylation of VE-cadherin and α-catenin leading to their dissociation and affecting endothelial AJ and its barrier function. Interestingly, cholesterol crystals also activated Frk in the stimulation of tyrosine phosphorylation of VE-cadherin and α-catenin leading to their dissociation and affecting endothelial AJ and its barrier function.

Many studies have shown that H_2O_2 acts as a signaling molecule, particularly via its capacity to influence PTK activation in response to a variety of stimulants [47, 48]. In this regard, it is interesting to note that cholesterol crystals trigger H_2O_2 production via XO-dependent manner. Furthermore, the observations that Allopurinol, an inhibitor of XO, suppresses cholesterol crystals-induced Frk activation, VE-cadherin and α-catenin tyrosine phosphorylation and their dissociation from each other restoring endothelial AJ integrity and barrier function suggest that XO-mediated H_2O_2 production is required for cholesterol crystals-induced endothelial AJ disruption and barrier dysfunction. Many reports have shown that endogenously derived metabolites of omega-3 fatty acids, namely resolvins promote resolution of inflammation [35–37]. These molecules have also been reported to exhibit protective effects against atherosclerosis [49, 50]. Furthermore, it was shown that the cellular levels of these lipid molecules deplete during the development of atherosclerotic lesions [51]. In addition, it was demonstrated that RvD1, the metabolite of DHA, while enhancing anti-inflammatory cytokine expression, promoting phagocytosis and inhibiting pro-inflammatory cytokine expression/secretion suppresses proinflammatory cellular actions such as neutrophil migration, PMN infiltration into the inflamed tissues and their activation as well as ROS production [37, 52–54]. Supporting the role of these lipid mediators in the resolution of inflammation, it was further reported that RvD1 protects endothelial TJ and its barrier function from LPS-induced disruption [55, 56]. In this context, our findings show that RvD1 protects endothelial AJ and its barrier function from cholesterol crystals-induced disruption. Specifically, RvD1 was found to block cholesterol crystals-induced H_2O_2 production, Frk activation, VE-cadherin and α-catenin tyrosine phosphorylation and their dissociation from each other, thereby restoring endothelial AJ integrity and its barrier function.

Oxidation of PTP catalytic cysteine residues leads to their inactivation [47, 48]. In the present study, we show that cholesterol crystals inactivate SHP2 via xanthine oxidase-mediated H_2O_2 production and oxidation of its catalytic cysteine residue. Consistent with its effect on H_2O_2 production, RvD1 also suppressed SHP2 cysteine oxidation and its inactivation. These observations along with the lack of the capacity of RvD1 in the suppression of Frk activation and VE-cadherin and α-catenin tyrosine phosphorylation and their dissociation, endothelial AJ disruption and its barrier dysfunction while SHP2 was inhibited pharmacologically suggest that the protective effects of RvD1 on endothelial AJ integrity and its barrier function require SHP2 activity. In other words, protection of SHP2 from oxidative inactivation is the underlying mechanism of RvD1 in the suppression of Frk activation, VE-cadherin and α-catenin tyrosine phosphorylation and their dissociation and endothelial AJ disruption and its barrier dysfunction. These findings also infer that the effects of cholesterol crystals on Frk activation, VE-cadherin and α-catenin tyrosine phosphorylation and their dissociation and endothelial AJ disruption and its barrier dysfunction were due to its ability of inhibition of SHP2. If it was true, then one would

expect that inhibition of SHP2 alone should enhance tyrosine phosphorylation of VE-cadherin and α-catenin, which was no the case. Based on these findings, it appears that besides SHP2 inactivation, blockade of other PTPs may also be involved in cholesterol crystals-induced VE-cadherin and α-catenin tyrosine phosphorylation and endothelial AJ disruption. The present observations also reveal that feeding mice with CRD induces XO expression and H_2O_2 production, SHP2 cysteine oxidation and its inactivation, Frk activation, VE-cadherin and α-catenin tyrosine phosphorylation and their dissociation from each other, endothelial AJ disruption and vascular permeability and RvD1 protects mice against all these adverse effects of CRD. RvD1 has been reported to protect both epithelial and endothelial barrier integrity in a murine model of hydrochloric acid-induced acute lung injury (57). Based on all these observations, it is likely that cholesterol crystals mimic LPS in the disruption of endothelial AJ and its barrier function and RvD1 exerts its protective effects via guarding PTPs such as SHP2 from inactivation by H_2O_2. In addition, these findings suggest that while inflammatory cues such as LPS and cholesterol crystals are inducing the disruption of endothelial cell-to-cell junctions and its barrier function, the antiinflammatory lipid mediators such as RvD1 suppress these effects at the level of ROS production and PTP inactivation.

ACKNOWLEDGEMENTS

This work was supported by a grant HL074860 from NHLBI to GNR.

REFERENCES

[1]. Aird WC, Phenotypic heterogeneity of the endothelium: I. Structure, function, and mechanisms, Circ. Res 100 (2007) 158–173. [PubMed: 17272818]

[2]. Pober JS, Sessa WC, Evolving functions of endothelial cells in inflammation, Nat. Rev. Immunol 7 (2007) 803–815. [PubMed: 17893694]

[3]. Vita JA, Keaney JF, Jr., Endothelial function: a barometer for cardiovascular risk? Circulation 106 (2002) 640–642. [PubMed: 12163419]

[4]. Bazzoni G, Dejana E, Endothelial cell-to-cell junctions: molecular organization and role in vascular homeostasis, Physiol. Rev 84 (2004) 869–901. [PubMed: 15269339]

[5]. Harris ES, Nelson WJ, VE-cadherin: at the front, center, and sides of endothelial cell organization and function, Curr. Opin. Cell Biol 22 (2010) 651–658. [PubMed: 20708398]

[6]. Mehta D, Malik AB, Signaling mechanisms regulating endothelial permeability, Physiol. Rev 86 (2006) 279–367. [PubMed: 16371600]

[7]. Dejana E, Giampietro C, Vascular endothelial-cadherin and vascular stability, Curr. Opin. Hematol 19 (2012) 218–223. [PubMed: 22395663]

[8]. Dejana E, Tournier-Lasserve E, Weinstein BM, The control of vascular integrity by endothelial cell junctions: molecular basis and pathological implications, Dev. Cell 16 (2009) 209–221. [PubMed: 19217423]

[9]. Baumer Y, McCurdy S, Weatherby TM, Mehta NN, Halbherr S, Halbherr P, Yamazaki N, Boisvert WA, Hyperlipidemia-induced cholesterol crystal production by endothelial cells promotes atherogenesis, Nat. Commun 8 (2017) 1129. [PubMed: 29066718]

[10]. Dejana E, Orsenigo F, Lampugnani MG, The role of adherens junctions and VE-cadherin in the control of vascular permeability, J. Cell Sci 121 (2008) 2115–2122. [PubMed: 18565824]

[11]. Esser S, Lampugnani MG, Corada M, Dejana E, Risau W, Vascular endothelial growth factor induces VE-cadherin tyrosine phosphorylation in endothelial cells, J. Cell Sci 111 (1998) 1853–1865. [PubMed: 9625748]

[12]. Andriopoulou P, Navarro P, Zanetti A, Lampugnani MG, Dejana E, Histamine induces tyrosine phosphorylation of endothelial cell-to-cell adherens junctions, Arterioscler. Thromb. Vasc. Biol 19 (1999) 2286–2297. [PubMed: 10521356]

[13]. Yamamoto M, Ramirez SH, Sato S, Kiyota T, Cerny RL, Kaibuchi K, Persidsky Y, Ikezu T, Phosphorylation of claudin-5 and occludin by rho kinase in brain endothelial cells. Am. J. Pathol 172 (2008) 521–533. [PubMed: 18187566]

[14]. Kundumani-Sridharan V, Dyukova E, Hansen DE, 3rd, Rao GN, 12/15-Lipoxygenase mediates high-fat diet-induced endothelial tight junction disruption and monocyte transmigration: a new role for 15(S)-hydroxyeicosatetraenoic acid in endothelial cell dysfunction. J. Biol. Chem 288 (2013) 15830–15842. [PubMed: 23589307]

[15]. Chattopadhyay R, Dyukova E, Singh NK, Ohba M, Mobley JA, Rao GN, Vascular endothelial tight junctions and barrier function are disrupted by 15(S)-hydroxyeicosatetraenoic acid partly via protein kinase C epsilon-mediated zona occludens-1 phosphorylation at threonine 770/772, J. Biol. Chem 289 (2014) 3148–3163. [PubMed: 24338688]

[16]. Chattopadhyay R, Tinnikov A, Dyukova E, Singh NK, Kotla S, Mobley JA, Rao GN, 12/15-Lipoxygenase-dependent ROS production is required for diet-induced endothelial barrier dysfunction, J. Lipid Res 56 (2015) 562–577. [PubMed: 25556764]

[17]. Broman MT, Kouklis P, Gao X, Ramchandran R, Neamu RF, Minshall RD, Malik AB, Cdc42 regulates adherens junction stability and endothelial permeability by inducing alphα-catenin interaction with the vascular endothelial cadherin complex. Circ. Res 98 (2006) 73–80. [PubMed: 16322481]

[18]. Abela GS, Aziz K, Vedre A, Pathak DR, Talbott JD, Dejong J, Effect of cholesterol crystals on plaques and intima in arteries of patients with acute coronary and cerebrovascular syndromes, Am. J. Cardiol 103 (2009) 959–968. [PubMed: 19327423]

[19]. Abela GS, Kalavakunta JK, Janoudi A, Leffler D, Dhar G, Salehi N, Cohn J, Shah I, Karve M, Kotaru VPK, Gupta V, David S, Narisetty KK, Rich M, Vanderberg A, Pathak DR, Shamoun FE, Frequency of Cholesterol Crystals in Culprit Coronary Artery Aspirate During Acute Myocardial Infarction and Their Relation to Inflammation and Myocardial Injury, Am. J. Cardiol 120 (2017) 1699–1707. [PubMed: 28867129]

[20]. Kataoka Y, Puri R, Hammadah M, Duggal B, Uno K, Kapadia SR, Tuzcu EM, Nissen SE, Nicholls SJ, Cholesterol crystals associate with coronary plaque vulnerability in vivo, J. Am. Coll. Cardiol 65 (2015) 630–632. [PubMed: 25677323]

[21]. Chen Z, Ichetovkin M, Hailman E, Cholesterol in human atherosclerotic plaque is a marker for underlying disease state and plaque vulnerability, Lipids Health Dis. 9 (2010) 61–68. [PubMed: 20540749]

[22]. Duewell P, Kono H, Rayner KJ, Sirois CM, Vladimer G, Bauernfeind FG, Abela GS, Franchi L, Nunez G, Schnurr M, Espevik T, Lien E, Fitzgerald KA, Rock KL, Moore KJ, Wright SD, Hornung V, Latz E, NLRP3 inflammasomesare required for atherogenesis and activated by cholesterol crystals, Nature 464 (2010) 1357–1361. [PubMed: 20428172]

[23]. Abderrazak A, Couchie D, Mahmood DF, Elhage R, Vindis C, Laffargue M, Matéo V, Büchele B, Ayala MR, El Gaafary M, Syrovets T, Slimane MN, Friguet B, Fulop T, Simmet T, El Hadri K, Rouis M, Anti-inflammatory and antiatherogenic effects of the NLRP3 inflammasome inhibitor arglabin in ApoE2.Ki mice fed a high-fat diet, Circulation 131 (2015) 1061–1070. [PubMed: 25613820]

[24]. Kotla S, Singh NK, Rao GN, ROS via BTK-p300-STAT1-PPARγ signaling activation mediates cholesterol crystals-induced CD36 expression and foam cell formation, Redox Biol. 11 (2017) 350–364. [PubMed: 28040583]

[25]. Gimbrone MA, Jr, García-Cardeña G, Endothelial Cell Dysfunction and the Pathobiology of Atherosclerosis, Circ. Res 118 (2016) 620–636. [PubMed: 26892962]

[26]. Rao RM, Yang L, Garcia-Cardena G, Luscinskas FW, Endothelial-dependent mechanisms of leukocyte recruitment to the vascular wall, Circ. Res 101 (2007) 234–247. [PubMed: 17673684]

[27]. McNamara DJ, Dietary cholesterol and atherosclerosis, Biochim. Biophys. Acta 1529 (2000) 310–320. [PubMed: 11111098]

[28]. Libby P, Inflammation in atherosclerosis, Nature 420 (2002) 868–874. [PubMed: 12490960]

[29]. Chandrasekharan S, Qiu TH, Alkharouf N, Brantley K, Mitchell JB, Liu ET, Characterization of mice deficient in the Src family nonreceptor tyrosine kinase Frk/rak, Mol. Cell. Biol 22 (2002) 5235–5247. [PubMed: 12077350]

[30]. Chattopadhyay R, Raghavan S, Rao GN, Resolvin D1 via prevention of ROS-mediated SHP2 inactivation protects endothelial adherens junction integrity and barrier function, Redox Biol. 12 (2017) 438–455. [PubMed: 28319894]

[31]. Guthikonda S, Sinkey C, Barenz T, Haynes WG, Xanthine oxidase inhibition reverses endothelial dysfunction in heavy smokers, Circulation 107 (2003) 416–421. [PubMed: 12551865]

[32]. Cai H, Harrison DG, Endothelial dysfunction in cardiovascular diseases: the role of oxidant stress. Circ. Res 87 (2000) 840–844. [PubMed: 11073878]

[33]. Kevil CG, Oshima T, Alexander B, Coe LL, Alexander JS. H_2O_2-mediated permeability: role of MAPK and occludin, Am. J. Physiol. Cell. Physiol 279 (2000) C21–30. [PubMed: 10898713]

[34]. Butler R, Morris AD, Belch JJ, Hill A, Struthers AD, Allopurinol normalizes endothelial dysfunction in type 2 diabetics with mild hypertension, Hypertension 35 (2000) 746–751. [PubMed: 10720589]

[35]. Levy BD, Clish CB, Schmidt B, Gronert K, Serhan CN, Lipid mediator class switching during acute inflammation: signals in resolution, Nat. Immunol 2 (2001) 612–619. [PubMed: 11429545]

[36]. Serhan CN, Hong S, Gronert K, Colgan SP, Devchand PR, Mirick G, Moussignac RL, Resolvins: a family of bioactive products of omega-3 fatty acid transformation circuits initiated by aspirin treatment that counter proinflammation signals, J. Exp. Med 196 (2002) 1025–1037. [PubMed: 12391014]

[37]. Bannenberg GL, Chiang N, Ariel A, Arita M, Tjonahen E, Gotlinger KH, Hong S, Serhan CN, Molecular circuits of resolution: formation and actions of resolvins and protectins, J. Immunol 174 (2005) 4345–4355. [PubMed: 15778399]

[38]. Juarez JC, Manuia M, Burnett ME, Betancourt O, Boivin B, Shaw DE, Tonks NK, Mazar AP, Doñate F, Superoxide dismutase 1 (SOD1) is essential for H2O2-mediated oxidation and inactivation of phosphatases in growth factor signaling, Proc. Natl. Acad. Sci. U. S. A 105 (2008) 7147–7152. [PubMed: 18480265]

[39]. Tabet F, Schiffrin EL, Callera GE, He Y, Yao G, Ostman A, Kappert K, Tonks NK, Touyz RM, Redox-sensitive signaling by angiotensin II involves oxidative inactivation and blunted phosphorylation of protein tyrosine phosphatase SHP-2 in vascular smooth muscle cells from SHR, Circ. Res 103 (2008) 149–158. [PubMed: 18566342]

[40]. Hellmuth K, Grosskopf S, Lum CT, Wurtele M, Roder N, von Kries JP, Rosario M, Rademann J, Birchmeier W, Specific inhibitors of the protein tyrosine phosphatase Shp2 identified by high-throughput docking, Proc. Natl. Acad. Sci. U.S.A 105 (2008) 7275–7280. [PubMed: 18480264]

[41]. Tabas I, Bornfeldt KE, Macrophage Phenotype and Function in Different Stages of Atherosclerosis, Circ. Res 118 (2016) 653–667. [PubMed: 26892964]

[42]. Birukova AA, Shah AS, Tian Y, Moldobaeva N, Birukov KG, Dual role of vinculin in barrier-disruptive and barrier-enhancing endothelial cell responses, Cell. Signal 28 (2016) 541–551. [PubMed: 26923917]

[43]. Baumeister U, Funke R, Ebnet K, Vorschmitt H, Koch S, Vestweber D, Association of Csk to VE-cadherin and inhibition of cell proliferation, EMBO J. 24 (2005) 1686–1695. [PubMed: 15861137]

[44]. Frye M, Dierkes M, Küppers V, Vockel M, Tomm J, Zeuschner D, Rossaint J, Zarbock A, Koh GY, Peters K, Nottebaum AF, Vestweber D, Interfering with VE-PTP stabilizes endothelial junctions in vivo via Tie-2 in the absence of VE-cadherin, J. Exp. Med 212 (2015) 2267–2287. [PubMed: 26642851]

[45]. Ukropec JA, Hollinger MK, Salva SM, Woolkalis MJ, SHP2 association with VE-cadherin complexes in human endothelial cells is regulated by thrombin, J. Biol. Chem 275 (2000) 5983–5986. [PubMed: 10681592]

[46]. Orsenigo F, Giampietro C, Ferrari A, Corada M, Galaup A, Sigismund S, Ristagno G, Maddaluno L, Koh GY, Franco D, Kurtcuoglu V, Poulikakos D, Baluk P, McDonald D, Grazia Lampugnani M, Dejana E, Phosphorylation of VE-cadherin is modulated by haemodynamic forces and

contributes to the regulation of vascular permeability in vivo, Nat. Commun 3 (2012) 1208. [PubMed: 23169049]

[47]. Denu JM, Tanner KG, Specific and reversible inactivation of protein tyrosine phosphatases by hydrogen peroxide: evidence for a sulfenic acid intermediate and implications for redox regulation, Biochemistry 37 (1998) 5633–5642. [PubMed: 9548949]

[48]. Schieber M, Chandel NS, ROS function in redox signaling and oxidative stress, Curr. Biol 24 (2014) R453–462. [PubMed: 24845678]

[49]. Hasturk H, Abdallah R, Kantarci A, Nguyen D, Giordano N, Hamilton J, Van Dyke TE, Resolvin E1 (RvE1) Attenuates Atherosclerotic Plaque Formation in Diet and Inflammation-Induced Atherogenesis, Arterioscler. Thromb. Vasc. Biol 35 (2015) 1123–1133.

[50]. Viola J, Lemnitzer P, Jansen Y, Csaba G, Winter C, Neideck C, Silvestre-Roig C, Dittmar G, Doring Y, Drechsler M, Weber C, Zimmer R, Cenac N, Soehnlein O, Resolving Lipid Mediators Maresin 1 and Resolvin D2 Prevent Atheroprogression in Mice, Circ. Res 119 (2016) 1030–1038. [PubMed: 27531933]

[51]. Fredman G, Hellmann J, Proto JD, Kuriakose G, Colas RA, Dorweiler B, Connolly ES, Solomon R, Jones DM, Heyer EJ, Spite M, Tabas I, An imbalance between specialized pro-resolving lipid mediators and pro-inflammatory leukotrienes promotes instability of atherosclerotic plaques, Nat. Commun 7 (2016) 12859.

[52]. Titos E, Rius B, Gonzalez-Periz A, Lopez-Vicario C, Moran-Salvador E, Martinez-Clemente M, Arroyo V, Claria J, Resolvin D1 and its precursor docosahexaenoic acid promote resolution of adipose tissue inflammation by eliciting macrophage polarization toward an M2-like phenotype, J. Immunol 187 (2011) 5408–5418. [PubMed: 22013115]

[53]. Norling LV, Dalli J, Flower RJ, Serhan CN, Perretti M, Resolvin D1 limits polymorphonuclear leukocyte recruitment to inflammatory loci: receptor-dependent actions, Arterioscler. Thromb. Vasc. Biol 32 (2012) 1970–1978. [PubMed: 22499990]

[54]. Kasuga K, Yang R, Porter TF, Agrawal N, Petasis NA, Irimia D, Toner M, Serhan CN, Rapid appearance of resolvin precursors in inflammatory exudates: novel mechanisms in resolution, J. Immunol 181 (2008) 8677–8687. [PubMed: 19050288]

[55]. Xie W, Wang H, Wang L, Yao C, Yuan R, Wu Q, Resolvin D1 reduces deterioration of tight junction proteins by upregulating HO-1 in LPS-induced mice, Lab. Invest 93 (2013) 991–1000. [PubMed: 23857007]

[56]. Zhang X, Wang T, Gui P, Yao C, Sun W, Wang L, Wang H, Xie W, Yao S, Lin Y, Wu Q, Resolvin D1 reverts lipopolysaccharide-induced TJ proteins disruption and the increase of cellular permeability by regulating IkappaBalpha signaling in human vascular endothelial cells, Oxid. Med. Cell. Longev 2013 (2013) 185715.

[57]. Eickmeier O, Seki H, Haworth O, Hilberath JN, Gao F, Uddin M, Croze RH, Carlo T, Pfeffer MA, Levy BD, Aspirin-triggered resolvin D1 reduces mucosal inflammation and promotes resolution in a murine model of acute lung injury, Mucosal Immunol. 6 (2013) 256–266. [PubMed: 22785226]

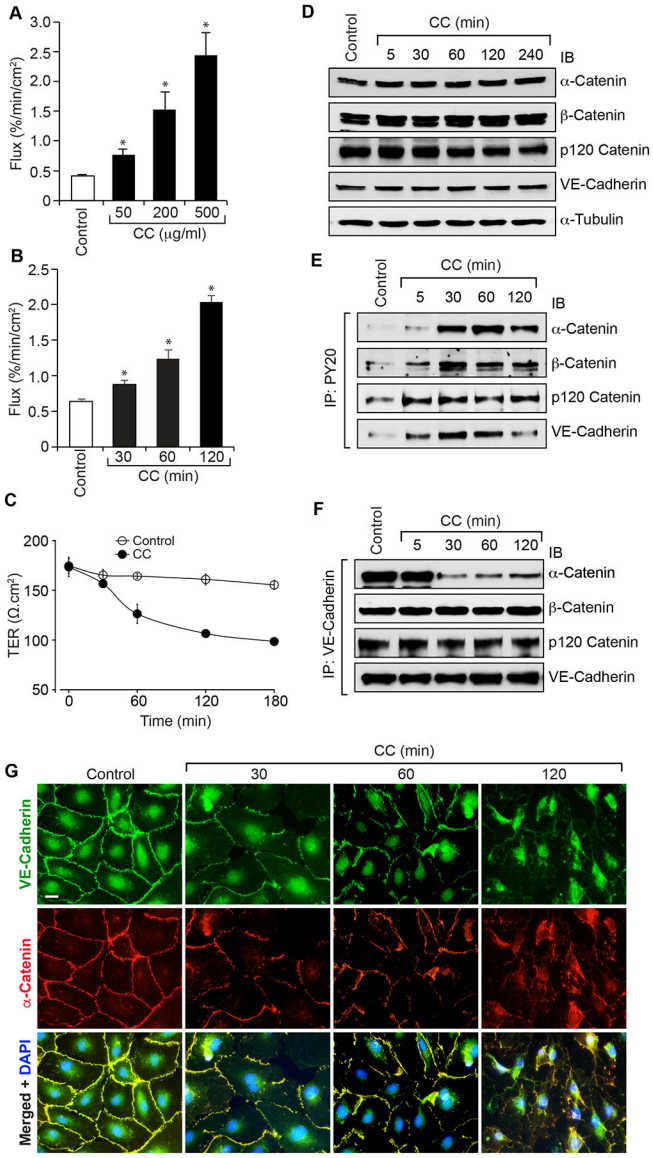

Figure 1. Cholesterol crystals disrupt endothelial AJ integrity and its barrier function.

A. Quiescent HAEC monolayer was treated with and without the indicated concentrations of cholesterol crystals for 2 hrs and flux was measured. B & C. Quiescent HAEC monolayer was treated with and without cholesterol crystals (200 mg/ml) for the indicated time periods and flux (B) and TER (C) were measured. D-F. Quiescent HAEC were treated with and without cholesterol crystals (200 mg/ml) for the indicated time periods, cell extracts were prepared and equal amounts of proteins from control and each treatment were either analyzed by Western blotting (IB) for the steady state levels of the indicated proteins (D) or immunoprecipitated (IP) with PY20 or VE-cadherin antibodies and the immunocomplexes were analyzed by immunoblotting (IB) for the indicated proteins (E & F) using their specific antibodies. G. Quiescent HAEC were treated with and without cholesterol crystals (200 μg/ml) for the indicated time periods and examined for AJ integrity by double immunofluorescence staining for VE-cadherin and α-catenin. Nucleus was stained with

DAPI. The bar graphs represent quantitative analysis of three experiments. The values are expressed as Means ± SD. *, $p < 0.05$ vs control.

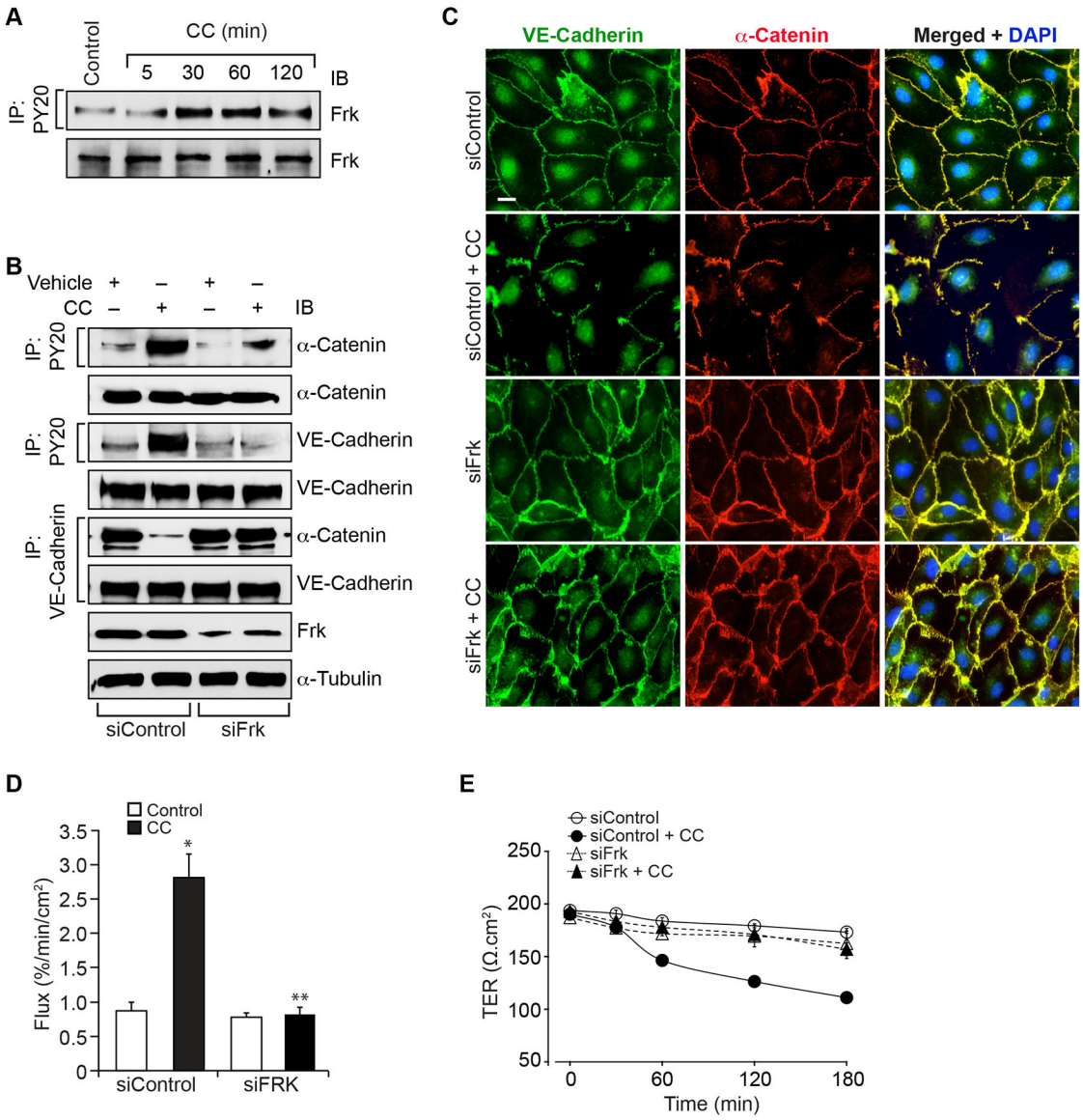

Figure 2. Frk mediates cholesterol crystals-induced endothelial AJ disruption its barrier dysfunction.

A. Quiescent HAEC were treated with and without cholesterol crystals (200 μg/ml) for the indicated time periods, cell extracts were prepared and equal amounts of proteins from control and each treatment were immunoprecipitated with PY20 antibodies and the immunocomplexes were analyzed by IB for Frk using its specific antibodies. The same cell extracts were analyzed by IB for total Frk levels. B. HAEC were transfected with siControl or siFrk, quiesced, treated with and without cholesterol crystals (200 μg/ml) for 30 min, cell extracts were prepared and equal amounts of proteins from control and each treatment were immunoprecipitated with PY20 or VE-cadherin antibodies and the immunocomplexes were analyzed by IB for the indicated proteins. The same cell extracts were also analyzed by IB for total VE-cadherin, α-catenin, Frk or α-tubulin levels to show the efficacy of the siRNAs on their target and off target molecules levels. C & D. All the conditions were the same as in panel B except that after 2 hrs, cells were either examined for AJ integrity by double

immunofluorescence staining for VE-cadherin and α-catenin (DAPI for nucleus) or subjected to flux analysis. E. All the conditions were the same as in panel B except that TER was measured at the indicated time periods. The bar graphs represent Mean ± SD values of three experiments, *, $p < 0.05$ vs siControl; **, $p < 0.05$ vs CC.

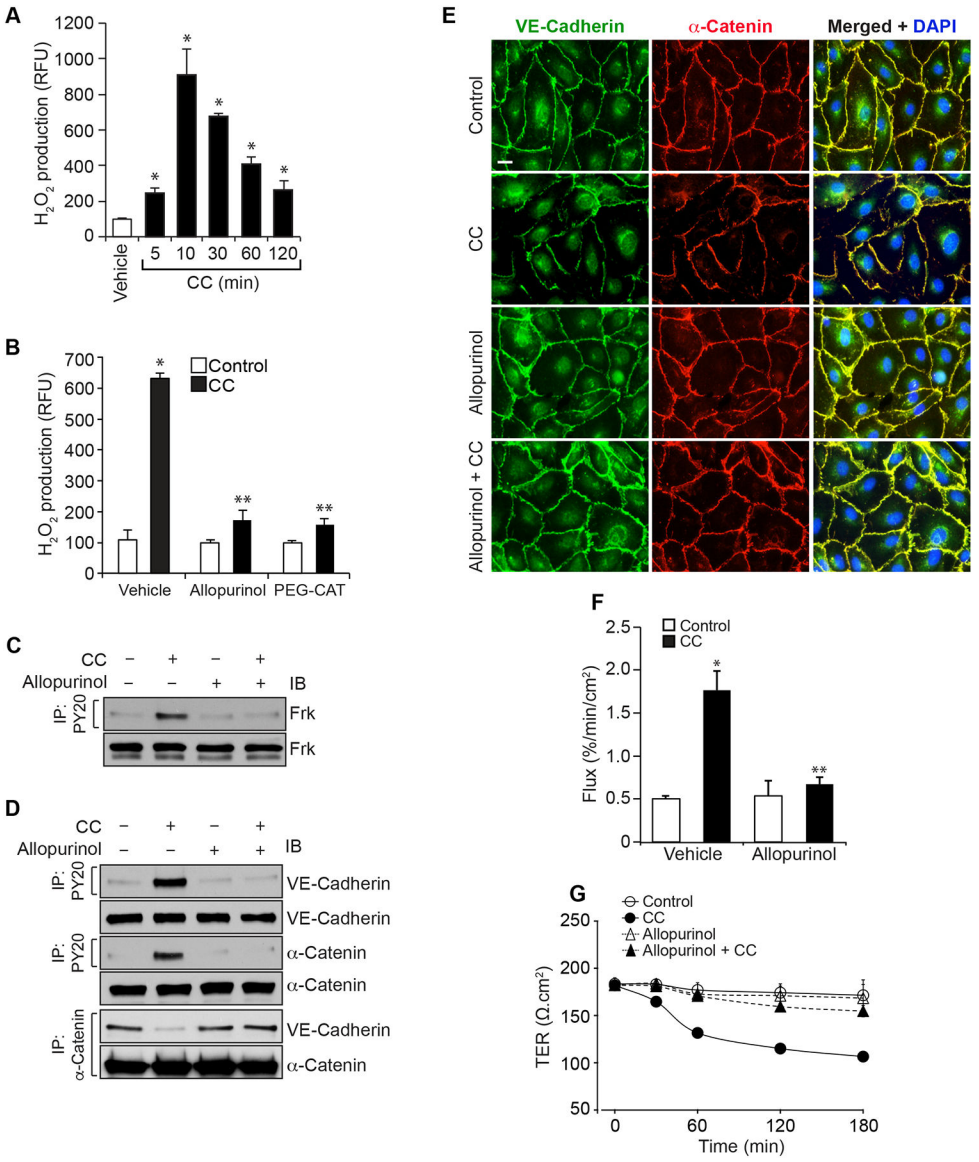

Figure 3. Cholesterol crystals-induced endothelial AJ disruption and its barrier dysfunction are required xanthine oxidase-mediated H_2O_2 production.

A. Quiescent HAEC were treated with and without CC (200 μg/ml) for the indicated time periods and H_2O_2 production was measured. B. Quiescent HAEC were treated with and without CC (200 μg/ml) in the presence and absence of Allopurinol (50 μM) or PEG-catalase (PEG-CAT) (100 U/ml) for 10 min and H_2O_2 production was measured. C & D. Quiescent HAEC were treated with and without CC (200 μg/ml) in the presence and absence of Allopurinol (50 μM) for 30 min and cell extracts were prepared. Equal amounts of proteins from control and each treatment were immunoprecipitated with PY20 or α-catenin antibodies and the immunocomplexes were analyzed by IB for the indicated proteins. The same cell extracts were also analyzed by IB for total Frk, VE-cadherin or α-catenin to show that the treatments do not affect their steady state levels. E & F. All the conditions were the same as in panel C except that after 2 hrs, cells were either examined for AJ integrity by double immunofluorescence staining for VE-cadherin and α-catenin (DAPI for nucleus) or

subjected to flux analysis. G. All the conditions were the same as in panel C except that TER was measured at the indicated time periods. The bar graphs represent Mean ± SD values of three experiments. *, $p < 0.05$ vs control; **, $p < 0.05$ vs CC.

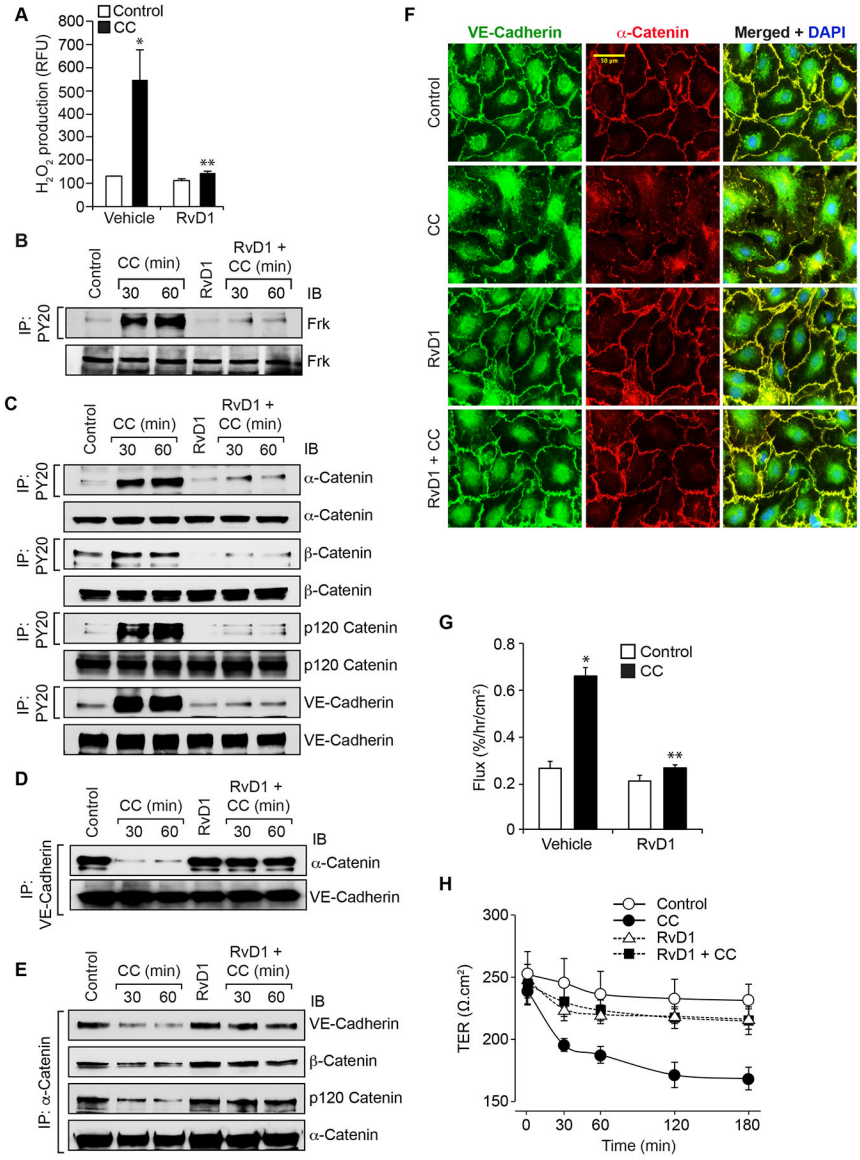

Figure 4. RvD1 inhibits cholesterol crystals-induced H_2O_2 production in suppressing Frk activation, AJ disruption and endothelial barrier dysfunction.

A. Quiescent HAEC were treated with and without CC (200 μg/ml) in presence and absence of RvD1 (200 ng/ml) for 10 min and H_2O_2 production was measured. B-E. Quiescent HAEC were treated with and without CC (200 μg/ml) in presence and absence of RvD1 (200 ng/ml) for the indicated time periods and cell extracts were prepared. Equal amounts of proteins from control and each treatment were immunoprecipitated with PY20, VE-cadherin or α-catenin antibodies and the immunocomplexes were analyzed by IB for the indicated proteins. The same cell extracts were also analyzed by IB for total Frk, α-catenin, β-catenin, p120 catenin or VE-cadherin to show that the treatments do not affect their steady state levels. F-H. Quiescent HAEC were treated with and without CC (200 mg/ml) in presence and absence of RvD1 (200 ng/ml) for 2 hrs and examined for either AJ integrity by double immunofluorescence staining for VE-cadherin and α-catenin (DAPI for nucleus) or subjected to flux assay or for the indicated time periods and TER was measured. The bar

graphs represent Mean ± SD values of three experiments. *, $p < 0.05$ vs control; **, $p < 0.05$ vs CC.

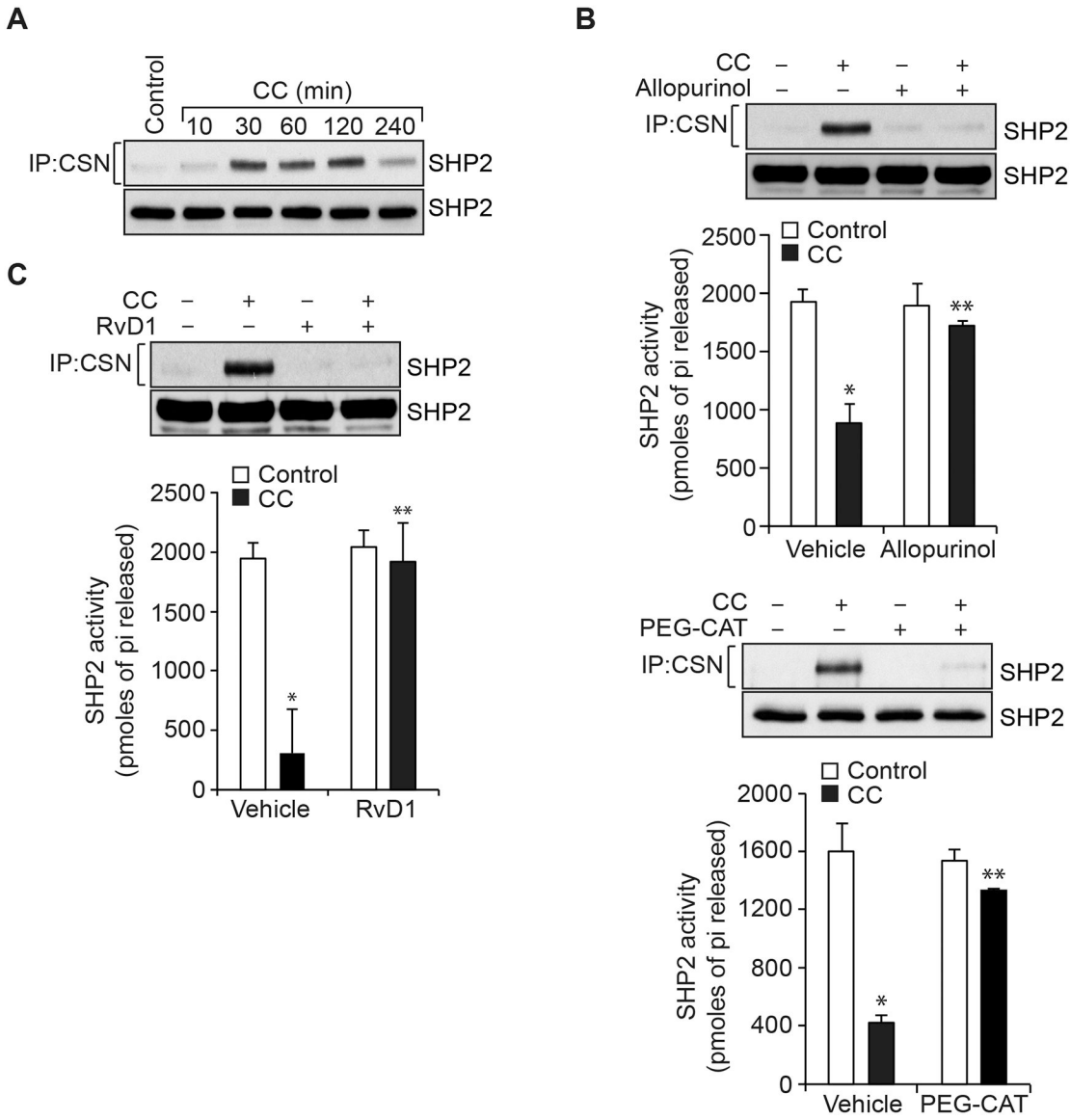

Figure 5. Cholesterol crystals via xanthine oxidase-mediated H_2O_2 production inhibits SHP2 activity.

A. Quiescent HAEC were treated with and without CC (200 μg/ml) for the indicated time periods, cell extracts were prepared and equal amounts of protein from control and each treatment were immunoprecipitated with cysteine sulfonate (CSN) antibodies and the immunocomplexes were analyzed by IB for SHP2 using its specific antibodies. The same cell extracts were also analyzed by IB for total SHP2 levels to show that the treatments do not affect its steady state levels. B & C. Quiescent HAEC were treated with and without CC (200 mg/ml) in the presence and absence of Allopurinol (50 μM), PEG-CAT (100 U/ml) or RvD1 (200 ng/ml) for 30 min, cell extracts were prepared and equal amounts of protein from control and each treatment were immunoprecipitated with CSN or SHP2 antibodies. Anti-CSN immunocomplexes were analyzed by IB for SHP2 levels using its specific antibodies and the anti-SHP2 immunocomplexes were analyzed for SHP2 activity. The bar graphs represent Mean ± SD values of three experiments. *, $p < 0.05$ vs control; **, $p < 0.05$ vs CC.

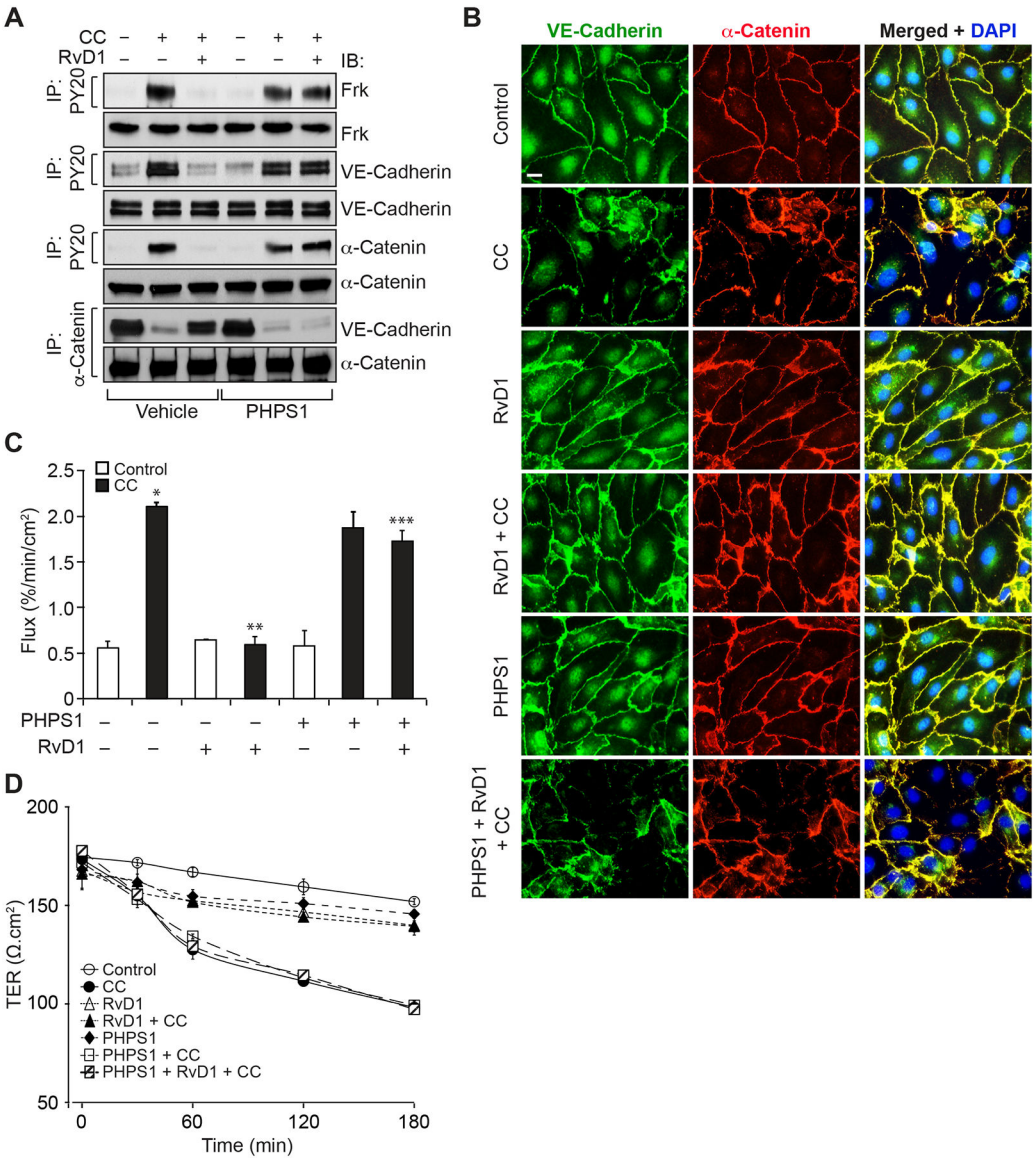

Figure 6. Pharmacological inhibition of SHP2 prevents the capacity of RvD1 in the attenuation of CC-induced Frk activation, VE-cadherin and α-catenin Tyr phosphorylation, AJ disruption and endothelial barrier dysfunction.

A. Quiescent HAEC were treated with and without CC (200 μg/ml) in the presence and absence of RvD1 (200 ng/ml) alone or in combination with or without PHPS1 (10 μM), a potent inhibitor of SHP2, for 30 min, cell extracts were prepared and an equal amount of protein from control and each treatment was immunoprecipitated with PY20 or α-catenin antibodies and the immunocomplexes were analyzed by IB for the indicated proteins. The same cell extracts were also analyzed for the indicated protein total Frk, VE-cadherin or α-catenin levels to show that the treatments do not affect their steady state levels. B & C. All the conditions were the same as in panel A except that after 2 hrs, cells were either examined for AJ integrity by double immunofluorescence staining for VE-cadherin and α-catenin (DAPI for nucleus) or subjected to flux analysis. D. All the conditions were the same as in panel A except that TER was measured at the indicated time periods. The bar graphs

represent Mean ± SD values of three experiments. *, $p < 0.05$ vs control; **, $p < 0.05$ vs CC; ***, $p < 0.05$ vs RvD1 + CC.

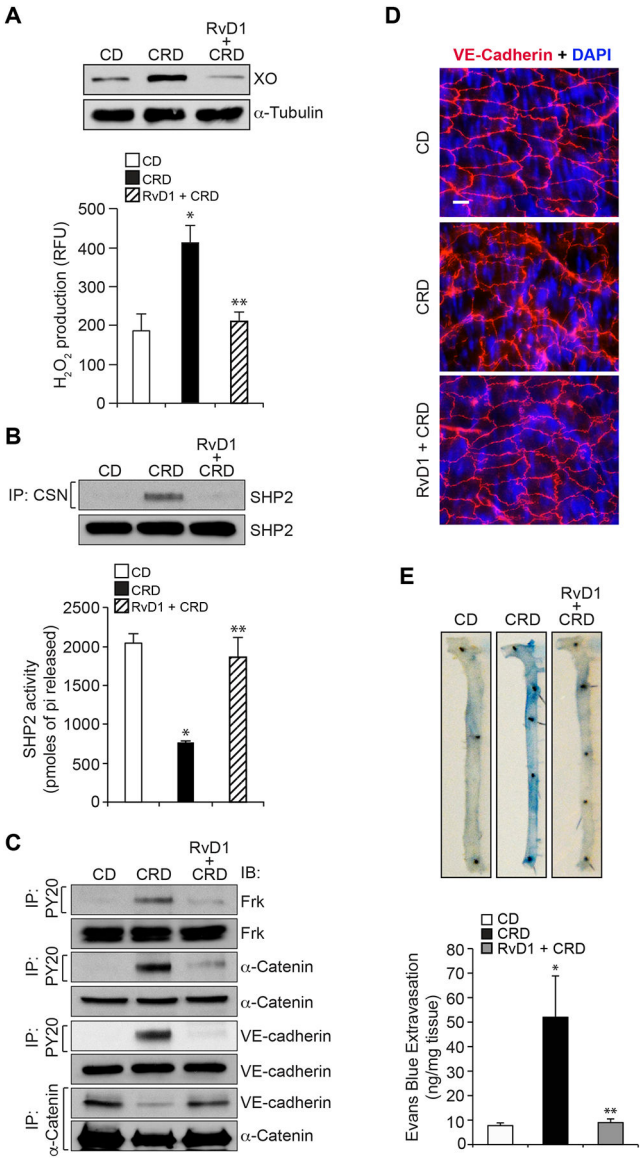

Figure 7. Cholesterol crystals increase vascular permeability by disrupting aortic endothelial AJ via H_2O_2-mediated SHP2 inactivation.

A. Eight weeks old C57BL/6 mice were fed with cholesterol rich diet (CRD) in combination with and without RvD1 (10 mg/kg body weight, every 2 days by IP) for 12 weeks, aortas were isolated and either tissue extracts were prepared and analyzed for XO expression by IB or minced and equal amounts were used to measure H_2O_2 levels by Amplex Red method. B. An equal amount of protein from aortic tissue extracts of the same regimen as in panel A were analyzed for SHP2 cysteine oxidation and its activity as described in Figure legend 5B. C. All the conditions were the same as in panel A except that tissue extracts containing an equal amount of protein from each regimen were immunoprecipitated with PY20 or α-catenin antibodies and the immunocomplexes were analyzed by IB for the indicated proteins using their specific antibodies. The same tissue extracts were also analyzed by IB for total Frk, α-catenin or VE-cadherin levels to show that the diet did not affect their steady state levels. D. All the conditions were same as in panel A except that after isolation the aortas

were opened longitudinally, fixed, permeabilized, blocked and immunostained for VE-cadherin (nucleus was stained with DAPI). E. All the conditions were the same as in panel A except that mice were anesthetized and 0.1 ml of 1% Evans Blue was injected via tail vein. After 20 min, the blood vessels were perfused with PBS through the left ventricle and the aortas were isolated and photographed. After taking the pictures, the aortas were minced, incubated in formamide solution at 55°C for 24 hrs, centrifuged and the optical density of the supernatant was measured at 610 nm in SpectraMax 190 spectrophotometer (Molecular Devices). The aortic endothelial barrier permeability was expressed as ng of Evans Blue extravasated per mg aorta. The bar graphs represent Mean ± SD values of three experiments with 2 animals/group or 6 animals minimum. *, $p < 0.05$ vs CD; **, $p < 0.05$ vs CRD.